

Ziziphus Jujube Seeds derived Biomass as Cost-Effective Biosorbent for the removal of Cr^{6+} from Aqueous solutions: Isotherm and Kinetic Studies

Ramesh Pandian R¹, Kalyani G², Gokulan R^{3*}, Anitha. A. S⁴

¹Department of Civil Engineering, University College of Engineering, Dindigul, Tamil Nadu

Email ID: rameshpandian999@gmail.com

²Department of Civil Engineering, Nadimpalli Satyanarayana Raju Institute of Technology,

Visakhapatnam, Andhra Pradesh – 531173, Email ID: kalyani.gaddam@gmail.com

³Department of Civil Engineering, GMR Institute of Technology, Rajam, Andhra Pradesh – 532

127, Email ID: gokulravi4455@gmail.com / gokulan.r@gmr.it.edu.in

⁴Department of Biotechnology, Karpaga Vinayaga College of Engineering and Technology,

Padalam, Tamil Nadu - 603308 Email Id: anithasnthl87@gmail.com

***Corresponding Author**

GRAPHICAL ABSTRACT



ABSTRACT

Biosorption of hexavalent chromium ions from the synthetic solution was performed using activated *Ziziphus jujube* seeds powder as an adsorbent material. A chemical synthesis process prepared the adsorbent, and various methods have evaluated its characteristics. FTIR, SEM and EDX analysis was conducted to check the ability of hexavalent chromium uptake from the synthetic solutions. Batch mode of adsorption process was performed and the adsorption parameters of pH, concentration, dose, contact time and temperature were found in various operating conditions. The entire adsorption process was evaluated by isotherm and kinetic models to check the nature of the adsorption process and its chemical reactions. Thermodynamic studies were conducted, desorption studies were used to recover the spent adsorbent using concentrated hydrochloric acid.

Keywords: *Batch adsorption, Ziziphus Jujube seeds, Hexavalent chromium, Isotherm studies, Kinetic studies.*

1. INTRODUCTION

Clean water is essential to all living beings for consumption and other usages. Water contamination is one of the new issues that we've been dealing with recently. Without clean water, the people and all living creatures cannot survive. Recently, water gets polluted due to various domestic and industrial activities. Due to the rapid population growth and their needs, the industries developed very high and created huge problems for the surroundings (Adeyemo et al, 2015). Tanneries, Electroplating, Dairy, fertilizers, Pulp & paper etc., are the various industries that release huge amounts of wastewater to produce their products. Among various industries, tanneries play an important role in water pollution (Labied et al, 2018). By processing the leather products, a huge amount of chromium metal ions was released into the water bodies through industrial effluent. During the chrome tanning process, the chromium ions have been converted into the hexavalent chromium (Cr^{6+}) stage, and it becomes highly toxic. Excess amounts of hexavalent chromium consumption may create toxic effects such as lung cancer and respiratory problems (Lucai et al, 2020). Hence, it is necessary to control chromium pollution in water using advanced treatment technologies. Many approaches are used to eliminate harmful pollutant concentrations from aqueous solutions. Chemical precipitation, Ion exchange, Membrane separation, and Adsorption are widely used to reduce the concentration of toxic pollutants in the

water. Among these, Adsorption is the process commonly used to reduce the concentration of heavy metals without the generation of any secondary pollutants and sludge (Khan et al, 2020).

Using the adsorbate material, the adsorption process produced very high removal efficiency from metal ion removal in wastewater. Many adsorbent substances were utilized to lower heavy metal ion concentrations in wastewater. Organic and inorganic adsorbents such as; banana peels, date seeds, fly ash, orange peels and sawdust powder were used to remove the heavy metal ions of Cu^{2+} , Pb^{2+} , Zn^{2+} and Hg^{2+} from the aqueous solutions (Amit Kumar et al, 2022). In this experimental work, Ziziphus Jujube (ZJ) seeds powder was used as an organic adsorbent material for removing the hexavalent chromium ion from the prepared synthetic solution. The ZJ seeds are commonly available in many places in India and are used for medical purposes. Various people are consuming these fruits and seeds to improve brain functions and the immunity powder against cancer and digestion. Many investigations have been carried out to extract heavy metal ions from aqueous solutions utilizing ZJ-based adsorbents. Table 1 represents the various researches works conducted using the ZJ adsorbent material and its capability for metal ion uptake from the aqueous solutions. In this study, ZJ seeds were transformed into activated carbon and employed as an adsorbent material to remove the hexavalent chromium (Cr^{6+}) ion from the synthetic solution. The maximum allowable limit of chromium ions in the drinking water is 100 $\mu\text{g/L}$, for sewage water 50 $\mu\text{g/L}$ and for water reuse 100 mg/L. All the experiments were performed in batch mode under various operating conditions, and multiple kinetic and thermodynamic approaches evaluated the adsorption process.

Table 1 – Research works conducted using ZJ based adsorbents

S. No.	Type of pollutant (s)	Metal ion uptake	Ion concentration	Ideal pH	ZJ adsorbent dose	Time of contact	Reference
1.	Cr^{6+}	63.23%	20 mg/L	2.0	0.6 g/L	50 min	In this study
2.	Cd^{2+}	49.40 mg/g	50 mg/L	2.0	1.6 g/L	40 min	Fakhar et al., 2021
3.	Cr^{6+}	62.08%	100 mg/L	2.0	1 g/L	120 min	Labied et al., 2018
4.	Cd^{2+} & Pb^{2+}	16.47 mg/g & 20.98 mg/g	70 mg/L	6.0	1 g	100 min	Khan et al., 2020
5.	As^{2+}	80%	50 ppb	4.5	0.3 mg/100ml	24 hours	Ziarati et al., 2019
6.	Humic acid	76.92 mg/g	50 mg/L	6.0	50 mg	300 min	Bouras et al., 2015

7.	Methylene Blue - Dye	88.77%	100 mg/L	4.0	1 g/L	30 min	Regti et al., 2017
----	-------------------------	--------	----------	-----	-------	--------	-----------------------

2. MATERIALS AND METHODS

2.1 Preparation ZJ seed adsorbent & stock solution

The ZJ seeds were collected from the trees and dried in sunlight for 24 hours to remove the water and moisture contents. The dried seeds are taken and ground well and converted into powder form. Using distilled water, the ZJ powder samples were washed several times to remove the impurities and placed in an oven at 100°C. After 8 hours, the sample was taken from the oven and concentrated sulfuric acid was added to make activated carbon ZJ seeds. The suspension was taken after 3 hours from the sulfuric acid using filter paper and again washed to remove the impurities. Then the sample was collected and used for another experimental purpose. The stock solution was prepared by adding 100 mg of potassium dichromate ($K_2Cr_2O_7$) powder with 1 litre of distilled water. With a known concentration of $K_2Cr_2O_7$ powder with distilled water, the experimental analysis was performed in batch mode.

2.2 Characterization of activated ZJ seeds

The specific surface area of activated ZJ seed powder and its pore structure was obtained using the nitrogen adsorption process at -196°C. The vacuum and gas molecules were removed from the activated ZJ seeds powder by keeping the powder at 300°C for 5 hours. The Brunauer-Emmett-Teller (BET) analysis was used to calculate the surface area (S_{BET}). The ZJ adsorbent surface's meso and micropore (S_u & S_m) area were calculated using the Dubinin–Radushkevich (D–R) relation of $S_m = S_{BET} - S_u$. The total pore (V_T) and liquid nitrogen volume were calculated under the high relation pressure of $P/P_o \sim 0.99$. The volume of micro and meso pores can be obtained by the $V_m = V_T - V_u$ relationship (Ziarati et al, 2019). The equation (1) for Barrett–Joyner–Halenda (BJH) model was used to evaluate the distribution of pores in activated ZJ seeds powder by taking the mean pore diameter (DP).

$$D_P = \frac{4 V_T}{S_{BET}} \quad (1)$$

The presence of functional groups in activated ZJ seeds adsorbent for adsorbing metal ions from the aqueous solutions was evaluated by Fourier Transform Infrared Spectroscopy (FTIR) analysis. To perform this analysis, the initial concentration of chromium synthetic solution was fixed at 20 mg/L with a pH of 6.0. 1 gm of activated ZJ seeds powder was added to that solution and placed in a rotary shaker. With 200 rpm of shaking for 3 hours, the final suspension was

taken and used for further experimental studies. The range for FTIR analysis was fixed from 400 – 4000 cm^{-1} with a scanning interval of 4 cm^{-1} resolution, and the scanning was performed up to 20 times. SEM analysis was performed with a working distance of 20 μm and a voltage level of 15 kV to confirm that adsorption occurs on the adsorbent surface. In order to determine the presence of hexavalent chromium ions on the activated ZJ seeds adsorbent, an Energy Dispersive X-Ray (EDX) analysis was performed using a SEM instrument.

2.3 Batch Adsorption studies

The batch studies of hexavalent chromium adsorption using activated ZJ seeds powder were performed by adjusting the parameters of pH, the concentration of chromium ions, ZJ seeds powder concentration, contact time between the ZJ seeds and chromium ions and temperature. By trial-and-error basis and literature reviews, the concentrations and levels of other parameters were adjusted, and the impact of chromium removal from the synthetic solution was evaluated. Using the pH buffer tablets, the solution's pH was adjusted from 2.0 to 7.0, and the solution's temperature was preserved at 30°C. The concentration of hexavalent chromium ions in the synthetic solution was adjusted to 20 - 100 mg/L, and the equilibrium time for complete adsorption reaction was allowed for up to 1 hour. To check the optimum ZJ seeds powder dose, the chromium concentration was fixed at 20 mg/L in 1 liter of distilled water, and the activated adsorbent dose was adjusted from 0.1 to 1 g/L. The contact time between adsorbent and metal ion was maintained between 30 to 180 minutes for 20 – 100 mg/L of varying chromium ion concentrations. For equilibrium attainment, the solution was kept in a rotary shaker for 60 minutes, the final suspension was taken after the batch adsorption studies, and the concentration was analyzed using AAS (Shimadzu – 6300). The concentration of metal ions before and after the adsorption process at the equilibrium time was calculated using equation 2.

$$q_t = \frac{(C_o - C_t) V}{m} \text{ mg/g} \quad (2)$$

The activated ZJ seeds charcoal powder and its metal ion uptake were denoted by q_t , and the concentration of batch adsorption study before and after hexavalent chromium uptake by activated ZJ seeds was denoted by C_o & C_t , respectively. The solution containing hexavalent chromium ions and its volume was denoted by V , and m represents the mass of the adsorption system. The equilibrium time was maintained at 30 minutes for each adsorption study, and the final suspension was taken after the equilibrium time and allowed for complete rest for 5

minutes. Then the concentration of the synthetic solution was examined using AA6300 spectrophotometric analysis. Each analysis was conducted up to 2 times to get the concurrent value of metal ion adsorption, and equation 3 was used to compute the adsorption system's mass balance method.

$$\% \text{ Removal} = \left[\frac{C_o - C_e}{C_o} \right] \times 100 \quad (3)$$

C_o & C_e represents synthetic solutions' initial and final metal ion concentrations.

2.4 Isotherm studies

The linear equation used to evaluate the transmission of adsorption from solution phase to adsorbent phase in equilibrium conditions is called the isotherm equation in adsorption studies (Batagarawa et al, 2019). Isotherm studies described the interaction of adsorbate molecules within the adsorption sites. At 30°C temperature with chromium ion concentration of 20 mg/L was taken for entire isotherm studies. The following common types of adsorption isotherm studies were used to check the performance of prepared activated ZJ seeds powder for hexavalent chromium removal from the aqueous solutions.

2.4.1 Langmuir isotherm study

The Langmuir isotherm study identified the equilibrium condition between the adsorbent phase and gas. Also, the relationship between solid and fluid interactions was observed by this isotherm model, and changes in the adsorption process were described (Bayuo et al, 2019). The Langmuir isotherm process follows the basic assumption of the monolayer adsorption process and its relative pressure under the nature of heterogeneous sites. Also, the binding process between the activated ZJ seeds and hexavalent chromium ions happened due to chemical reactions (Bouras et al, 2015). Equation 4 expresses the linear equation for the Langmuir isotherm model.

$$\frac{C_e}{q_e} = \frac{1}{K \cdot q_{max}} + \frac{C_e}{q_{max}} \quad (4)$$

Here, the concentration of metal ion solution during the equilibrium time was denoted by C_e , hexavalent chromium ions adsorbed per gram were denoted by q_e and the Langmuir isotherm constants were denoted by K & q_{max} for adsorption capacity and intensity, respectively.

2.4.2 Freundlich isotherm study

The amount of gas adsorbed by unit mass of activated ZJ seeds adsorbent and its variations were evaluated by the Freundlich isotherm study under the given temperature and system

pressure (Biswajit et al, 2011). This study allowed multiple adsorption layers on the activated ZJ seeds powder adsorbent, and the surface adsorption has developed by heterogeneous nature. Equation 5 expresses the linear equation for the Freundlich isotherm model.

$$\ln q_e = \ln k_f + \frac{1}{n} \ln C_e \quad (5)$$

Here, the quantity of adsorbed metal ions by ZJ seeds per gram was denoted by q_e ; the adsorption energy was denoted by n , the equilibrium concentration of metal ion-containing solution was denoted by C_e and Freundlich constant related to adsorption capacity was denoted by K_f .

2.4.3 Sips isotherm study

The heterogeneous sites were predicted by limiting behavior levels using the sips model, a combination of Langmuir and Freundlich model isotherms (Djelloul et al, 2014). This model did not consider the adsorbate concentration, and the monolayer adsorption process was followed. Equation 6 expresses the linear equation for the sips isotherm model.

$$\frac{1}{q_e} = \frac{1}{Q_{max}K_s} \left(\frac{1}{C_e} \right)^{\frac{1}{n}} + \frac{1}{Q_{max}} \quad (6)$$

Here, the capacity of adsorption was denoted by Q_{max} ; K_s represented the equilibrium constant, and the heterogeneity factor was denoted by n .

2.4.4 Toth isotherm study

The Langmuir isotherm model produces some discrepancies between equilibrium and experimental data. For reducing these discrepancies, Toth isotherm model has been used. The detailed description of adsorption process in low metal ion concentrations and higher metal ion uptake was described by this study (Ouyang et al, 2019). The linear equation for Toth isotherm model can be expressed in equation 7.

$$\ln \frac{q_e}{q_m - q_e} = n \ln K_L + n \ln C_e \quad (7)$$

Here, the metal ions adsorbed quantity in the equilibrium conditions was denoted by q_e and the Toth isotherm constants was denoted by K_L & n .

2.4.5 Redlich-Peterson (R-P) isotherm study

The R – P isotherm model, a three-parameter derived from Langmuir & Freundlich isotherm studies, followed the multilayer adsorption process. The basic assumption of this study is the

mechanism between metal ions and activated ZJ seeds adsorbent is unique and does not follow any monolayer adsorption process (Edidiong et al, 2018). Equation 8 expresses the linear equation of the R-P isotherm model.

$$\ln(K_R \frac{C_e}{q_e} - 1) = b_R \ln C_e + \ln a_R \quad (8)$$

Here, the adsorption capacity constant is denoted by K_R , a_R denote the R-P isotherm constant, and b_R denotes the exponent value.

2.5 Kinetic studies

For optimizing the adsorbent material and the interaction between metal ions and activated ZJ seeds was analyzed in kinetic studies. The kinetic models are used to evaluate the performance of activated ZJ seeds adsorbent and mass transfer mechanisms (Regti et al, 2017). The following kinetic studies are commonly used to evaluate the process of adsorption using adsorbent material.

2.5.1 Pseudo first order study

The capacity of solid adsorption was established within the liquid, and solid systems were examined by Pseudo first order or Lagergren model. The desorption rate of metal ions is directly proportional to the driving force (Francisco et al, 2020). The metal ion uptake by activated ZJ seeds powder was identified using the difference of initial (q_e) and equilibrium (q) concentrations of metal ion-containing solution. The equation for Lagergren kinetic model can be expressed in equation 9.

$$\frac{dq_e}{dq_t} = k (q_e - q_t) \quad (9)$$

Calculating the q_e & q_t values, the volume of chromium uptake by ZJ seeds adsorbent at any time (t) was obtained in an equilibrium state. Applying the boundary conditions and equation 9 can be rearranged to equation 10.

$$\log(q_e - q) = \log q_e - \frac{k}{2.303} t \quad (10)$$

2.5.2 Pseudo second order study

The assumption of this kinetic model is that the availability of empty sites in the activated ZJ powder adsorbent is directly proportional to the adsorption rate (Boubaker et al, 2021). The pseudo-second-order kinetic model can be represented using the assumption in equation 11.

$$\frac{dq}{dt} = k(q_e - q)^2 \quad (11)$$

By applying boundary conditions ($t = 0$ to $t > 0$, and $q = 0$ to $q > 0$), the Equation 11 can be rearranged as Equation 12.

$$\frac{t}{q} = \frac{1}{h} + \frac{1}{q_e} t \quad (12)$$

Here, the initial adsorption rate was denoted by $h = kq_e^2$, rate constant was denoted by k .

2.5.3 Elovich Kinetic study

During the initial stages of the adsorption process, The Elovich kinetic model was used to assess the chemical adsorption of gas molecules on the adsorbent's solid surface (Baidhani et al, 2016). The underlying assumption of this kinetic analysis was that the amount of adsorbed solute increased exponentially as the rate of adsorption decreased. Equation 13 represents the Elovich kinetic model.

$$\frac{d q_t}{d t} = a \exp (-b q_t) \quad (13)$$

Here, the Elovich model parameters were denoted by a & b in mg/g & g/mg , respectively. The boundary conditions of $q = 0$ at $t = 0$ and $q_t = q_t$ at $t = t$ was applied in equation 13, and the Elovich rate model can be expressed in equation 14.

$$q_t = \frac{1}{b} \ln (1 + a b t) \quad (14)$$

3. RESULYTS AND DISCUSSION

3.1 FTIR STUDIES

Figure 1 (a) & (b) shows the FTIR peaks of raw and activated biochar ZJ seeds powder, respectively. Referring to the raw adsorbent powder, the maximum peak attained at 1602 cm^{-1} may confirm the presence of the carbonyl group and its ring vibration. Also, the maximum bandwidth was generated in the 3390 cm^{-1} , confirming the stretching functional groups of alcohol and water. The peak 3350 cm^{-1} was developed because of $-\text{CH}$ stretching, and no further peak development was observed. The activated ZJ powder and its peaks (fig.1b) show the maximum number of peaks because of the presence of various functional groups. The peak at 2924 cm^{-1} indicates symmetrical bending due to the stretching of O-H groups. The $-\text{CH}_2$ bending vibrations were observed at the peak of 1595 cm^{-1} , and the peak disappears after 1092 cm^{-1} may confirm the $-\text{COO}$ stretching (Hong et al, 2020). The above experimental study shows evidence of the presence of organic functional groups to adsorb the pollutants from aqueous solutions.

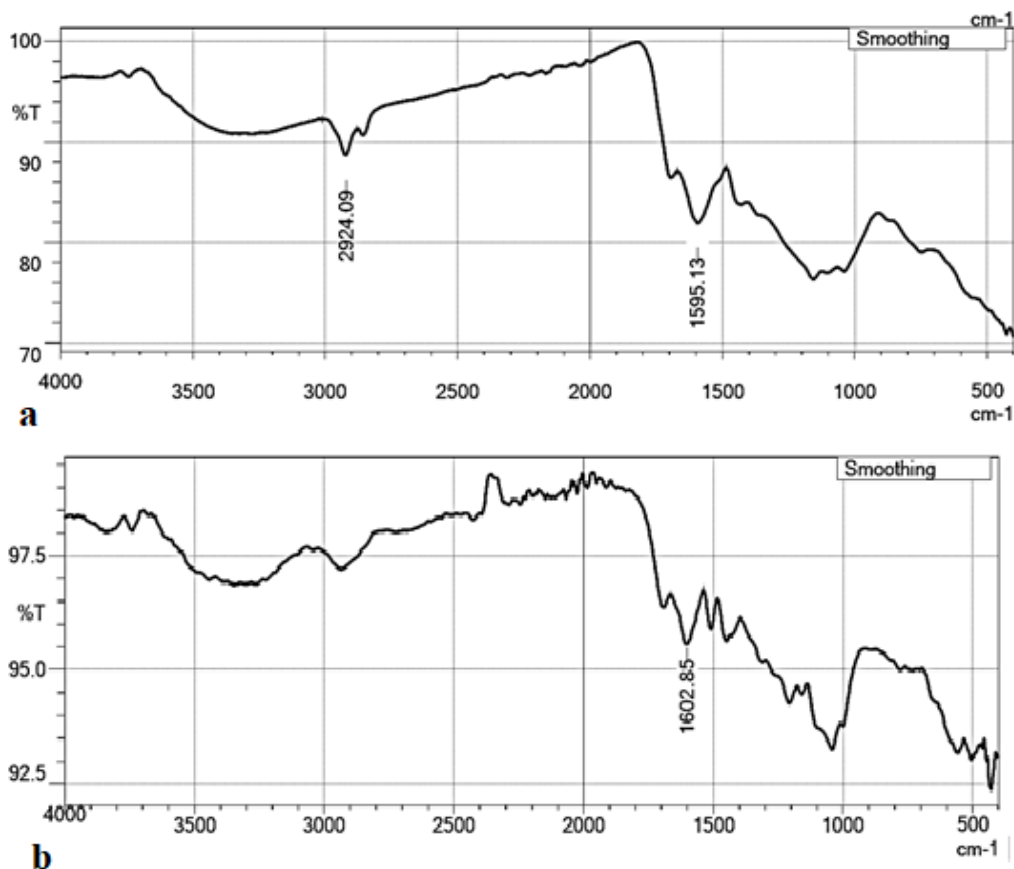


Figure 1 – FTIR analysis of (a) Raw ZJ seeds powder and (b) Activated ZJ seeds powder

3.2 SURFACE AREA AND PORE DISTRIBUTION

The process of adsorption-desorption isotherm was used to check the pore size and surface area of prepared activated ZJ seeds powder under the temperature of -196°C. The adsorption-desorption isotherm curve of activated ZJ powder seeds was shown in figure 2, and it confirms the adsorption process follows type – II (both Micro & Meso pores) nature. The adsorbent produced micro pores and was exhibited in the first curve, and the second portion represents the meso pores in a high amount of relative pressure (Aswini et al, 2019). Table 2 represents the micro and meso pore values of adsorbent material along with its pore radius & surface area. The surface area of ZJ seeds powder is 4.75 m²/g which is lesser than normal activated carbons.

Table 2 - Pore characteristics of raw and activated ZJ seeds powder

S.No	Description	ZJ Activated Biochar - Characteristics
1.	BJH surface area (m ² /g)	76.983

2.	Pore volume (cc/g)	0.116
3.	Pore Radius (Å)	32.822
4.	BET surface area (m ² /g)	4.75
5.	Average pore diameter (nm)	0.006

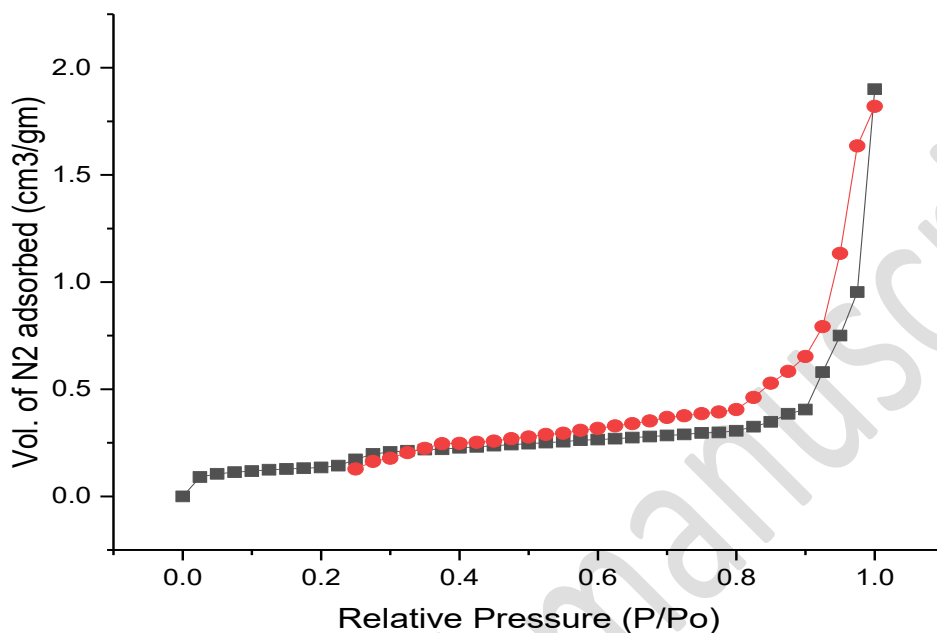


Figure 2 - BET isotherm study of activated ZJ seeds adsorbent by Nitrogen adsorption – desorption process

3.3 SEM EDX ANALYSIS

Scanning Electron Microscopic image of activated ZJ seeds powder before and after hexavalent chromium uptake from the synthetic solution was shown in figures 3 (a) & (b), respectively. The pores on activated ZJ seeds powder were developed by washing the adsorbent using concentrated sulfuric acid. Referring the figure 3 (a), the presence of pore was observed in a huge amount on the adsorbent's surface. These pores are very helpful in receiving the pollutants from the aqueous medium. Also, the adsorbent has a very large surface area and a high amount of active site availability. The metal ion-containing solution was passed into the activated ZJ adsorbent and the surface was examined by SEM analysis, as shown in figure 3 (b). The adsorbent's surface was filled with a lot of pollutants, and materials completely occupied the pores are seen in that figure 3 (b). The pollutants were filled and formed a cloud shape on the top side of the adsorbent's

surface. When the adsorption process was finished, the pollutant uptake by the adsorbent was reduced and attained the equilibrium stage (Luisa et al, 2018). Due to very high attraction forces and pollutants settlement on the inner walls of adsorbent materials, the presence of active sites was filled. Based on the SEM studies, the adsorption of pollutants by the activated ZJ seeds was confirmed. To ensure the hexavalent chromium ion adsorption by the adsorbent, EDX analysis were performed.

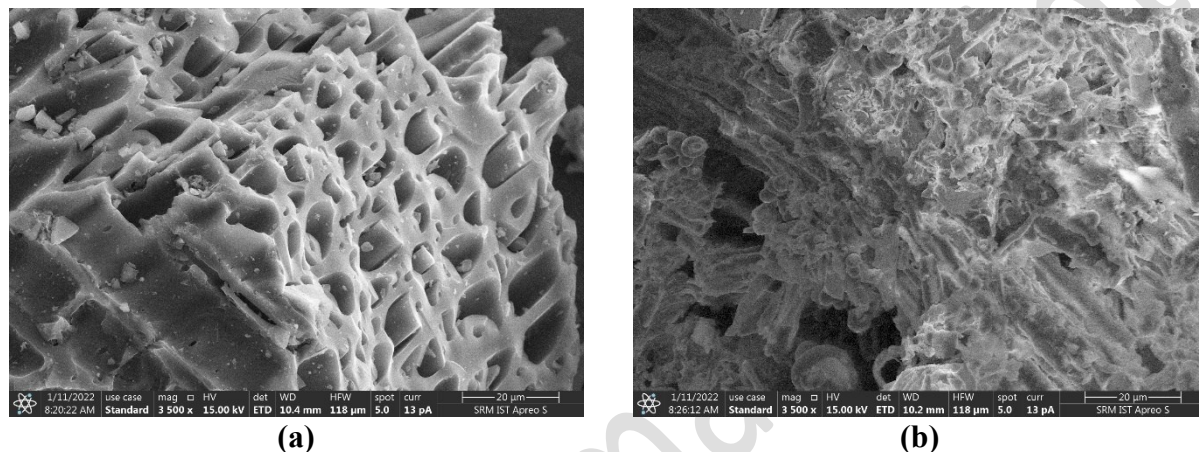


Figure 3 – SEM image of activated ZJ seeds powder (a) before Cr^{6+} uptake and (b) after Cr^{6+} uptake in batch adsorption

3.4 EDX ANALYSIS

The Energy Dispersive X-ray analysis of Activated ZJ seeds powder, before taking the hexavalent chromium ions and after taking the metal ions, is shown in figure 4 (a) & (b), respectively. The ZJ seeds powder before metal ion uptake from the synthetic solutions shows (fig. 4a) the presence of many organic and inorganic functional groups on the surface. The presence of carbon, aluminum, potassium and calcium elements was observed in figure 4a. On the other hand, figure 4b shows the presence of various pollutants and organic & inorganic elements after passing the chromium-containing solution into the activated ZJ powder adsorbent. Apart from the elements mentioned before the adsorption process, the presence of chromium ions was observed in figure 4b. Referring to the EDX analysis figures, it was confirmed the ability of the prepared adsorbent to remove the hexavalent chromium ions from the aqueous medium.

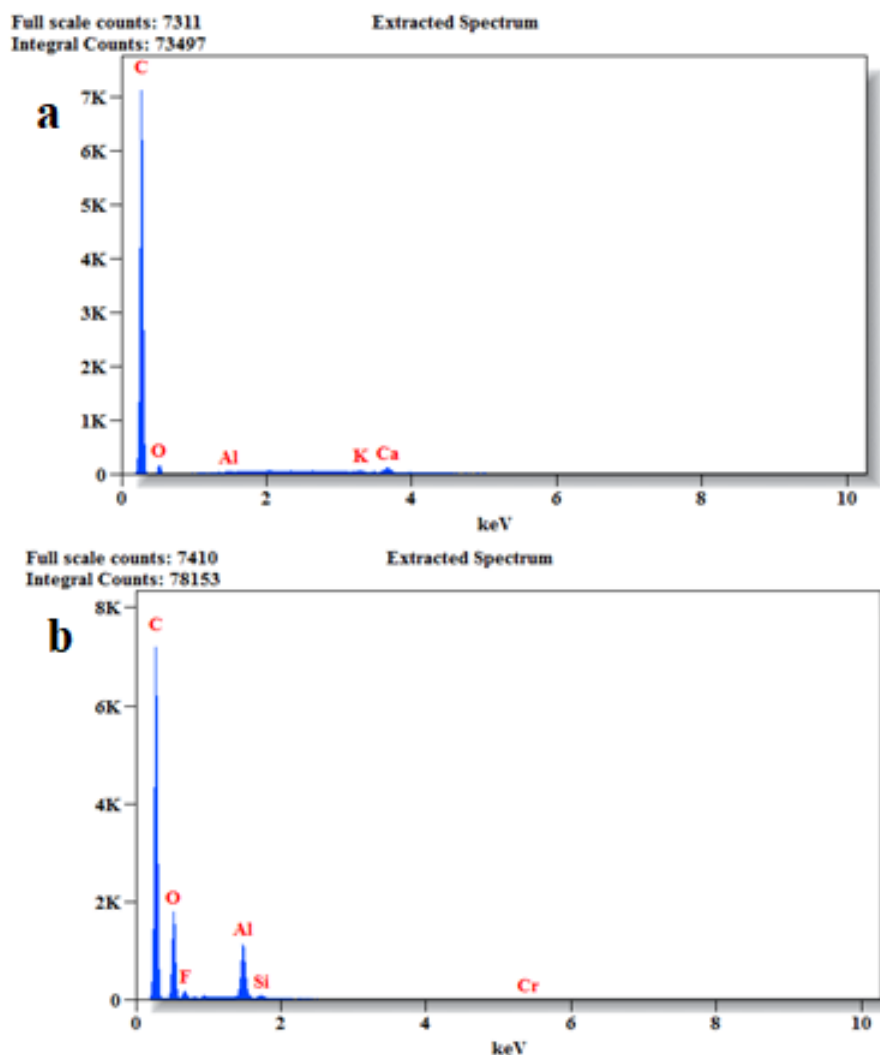


Figure 4 – EDX image of activated ZJ seeds powder (a) before Cr^{6+} uptake and (b) after Cr^{6+} uptake in batch adsorption

3.5 Impact of chromium uptake by varying the pH

Batch adsorption tests were carried out to test the effect of hexavalent chromium adsorption by altering the pH of the metal ion-containing solution from 2.0 to 7.0. Taking the initial concentration of the chromium-containing solution at 20 mg/L, activated ZJ seeds powder dose of 1 g/L, and contact time of 30 minutes, the experimental analysis was done at the temperature of 30°C. Figure 5 shows the impact of hexavalent chromium uptake by varying the pH of the synthetic solution. During the initial stages, the pH level is very low, the hexavalent chromium uptake by activated ZJ seeds powder is very high and attained the maximum adsorption rate. The negatively charged ions in low pH may attract the positively charged ions and increases the

metal ion interactions (Manjuladevi et al, 2018). When the pH of the metal ion-containing solution was increased, the decrease in the percentage of chromium adsorption was noticed in figure 5 (a). The adsorption decreased due to the hydroxide precipitation at higher pH levels. The maximum amount of 63.25% hexavalent chromium ions was removed at the optimum pH of 2.0.

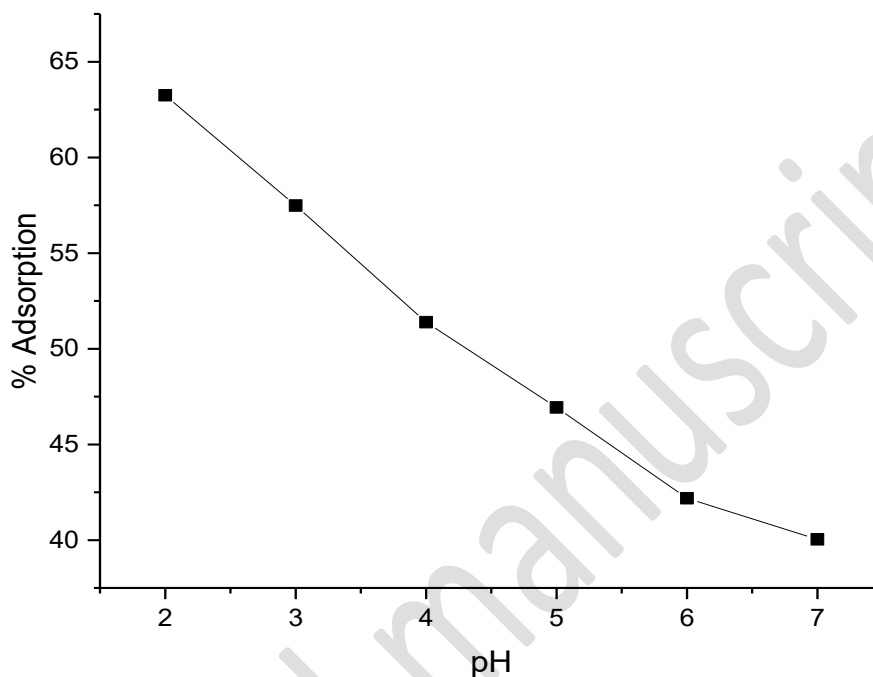


Figure 5 – Impact of chromium metal ion uptake by varying pH

3.6 Impact of chromium uptake by ZJ seeds dose

The activated ZJ powder dosage level was adjusted from 0.1 to 1 g/L, and the other parameters, such as chromium concentration in synthetic solution at 20 mg/L, contact time of 30 minutes and optimum pH of 2.0, were fixed. The impact of chromium adsorption was analyzed at the temperature of 30°C. Figure 6 shows the impact of hexavalent chromium ions uptake from the synthetic solution using activated ZJ adsorbent. There was an increase in the amount of chromium adsorption with an increase in adsorbent dosage has been noticed from the plot. Around 65.06 % of hexavalent chromium ions were observed in the aqueous solution taking the adsorbent dose of 0.6 g/L. A sudden decrease in metal ion adsorption was noticed with a further increase in adsorbent dose. The adsorbent dosage level is low, the active sites in the adsorbent's surface are reduced, and the pollutant uptake is considerably decreased (Feszterová, et al, 2021). The presence of active sites gets filled by the pollutants at an optimum level, and no further

decrease in metal ions uptake was noticed beyond 0.6 g/L. The concentration gradient was developed at high adsorbent dose levels may reduce the amount of adsorption after the optimum dose level.

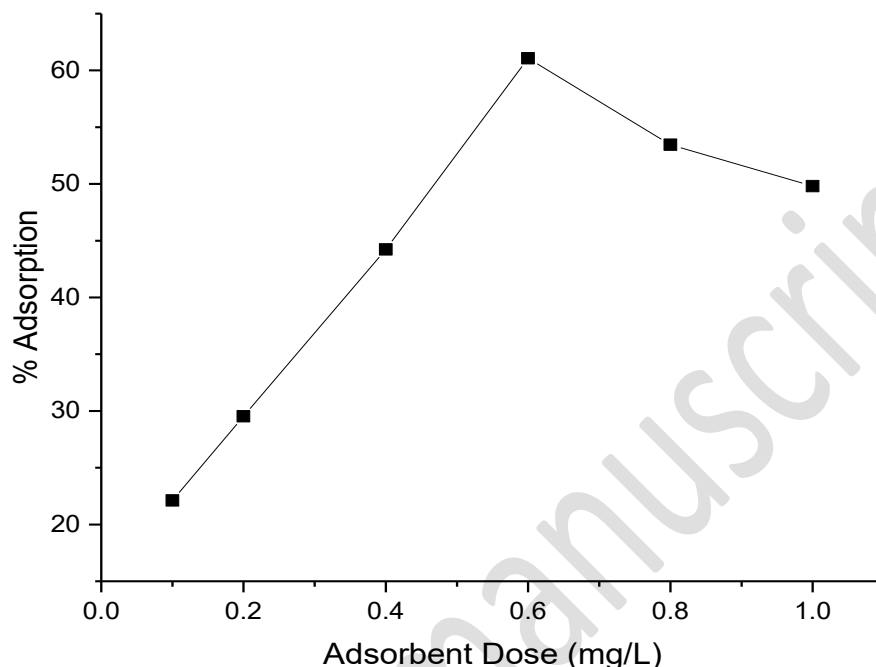


Figure 6 – Impact of chromium metal ion uptake by varying Adsorbent Dose

3.7 Impact of chromium uptake by metal ion concentration

The pH and adsorbent dose was fixed at 2.0 & 5 g/L, and the impact of hexavalent chromium ion uptake was analyzed by varying the synthetic solution's concentrations from 20 to 100 mg/L with 20 mg/L common intervals. Referring to figure 7, the metal ion uptake from the aqueous solution was very rapid during the starting stage. The chromium ion-containing solutions and their concentrations were increased, and there was a decrease in metal ion uptake. A sharp decrease was noticed with an increase in adsorbate concentrations in the aqueous solutions because of the high availability of pollutants and low availability of active sites (Saeed et al, 2020). The metal ion removal attained a saturation level with a further increase in adsorbent concentration. The activated carbon charcoal adsorbent provides a very high efficiency when the solution's concentration is very low. Based on the availability of active sites, the changes happened.

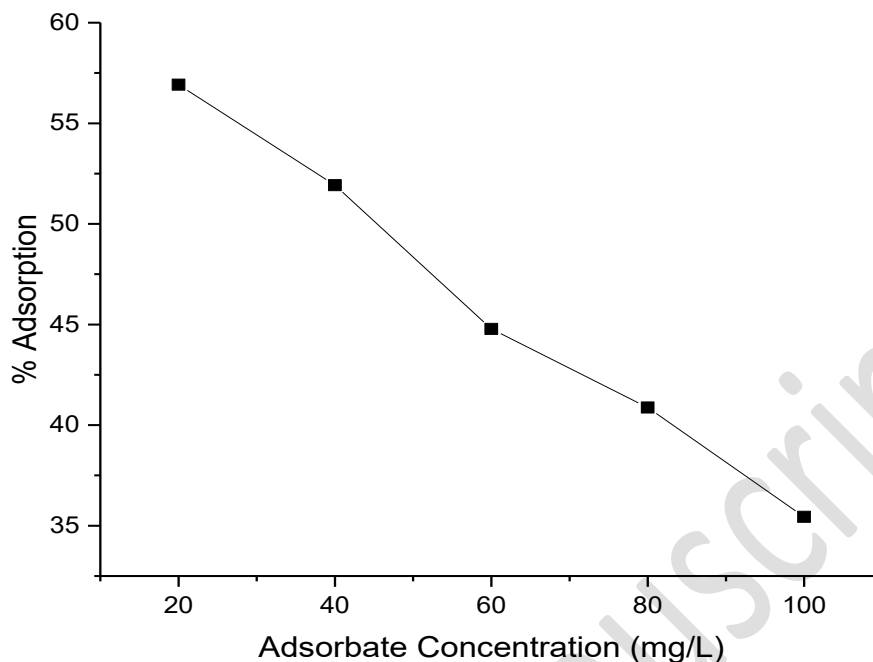


Figure 7 – Impact of chromium metal ion uptake by varying Adsorbate Concentration

3.8 Impact of chromium uptake by varying the contact time

By adjusting the starting chromium ion concentrations from 20 to 100 mg/L, the contact period between adsorbent and adsorbate was varied from 30 to 180 minutes. Figure 8 shows the variations in hexavalent chromium metal ion uptake by adjusting the contact time between chromium metal ions and activated ZJ seeds powder. During the initial stages, the chromium uptake by the adsorbent was rapid for all metal ion concentrated solutions, and the rate of adsorption reached the saturation level when the contact time reached 80 minutes. The vacant sites were filled with pollutants. After that, no vacant sites were available due to the repulsive force on the ZJ adsorbent molecule surface. Also, the pores in the adsorbent are much deeper, and the metal ions need to penetrate the pores with high force (Langeroodi et al, 2018). Because of this reason, the metal ion uptake by the adsorbent was reduced considerably.

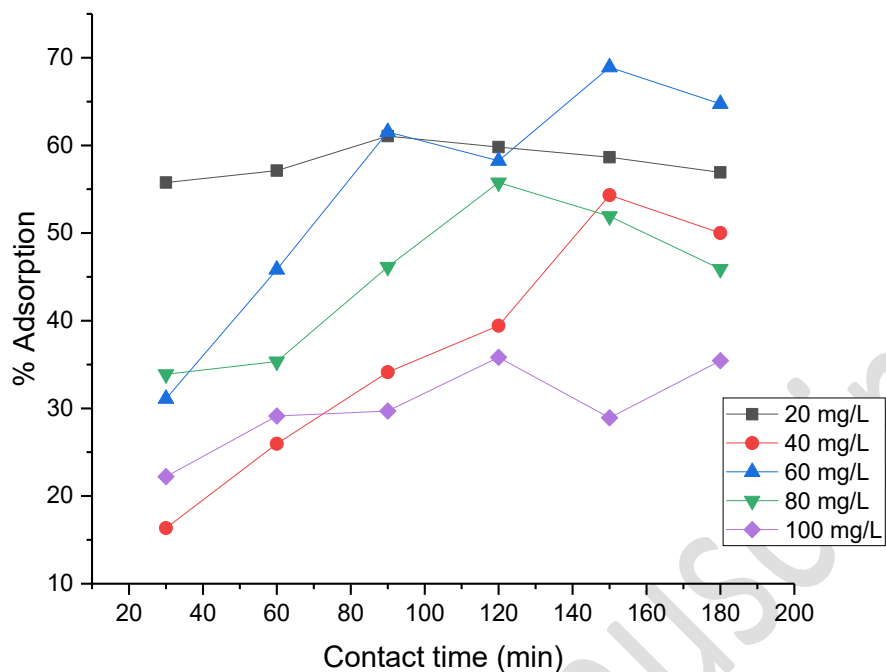


Figure 8 – Impact of chromium metal ion uptake by varying Contact Time

3.9 Impact of chromium uptake by varying the temperature

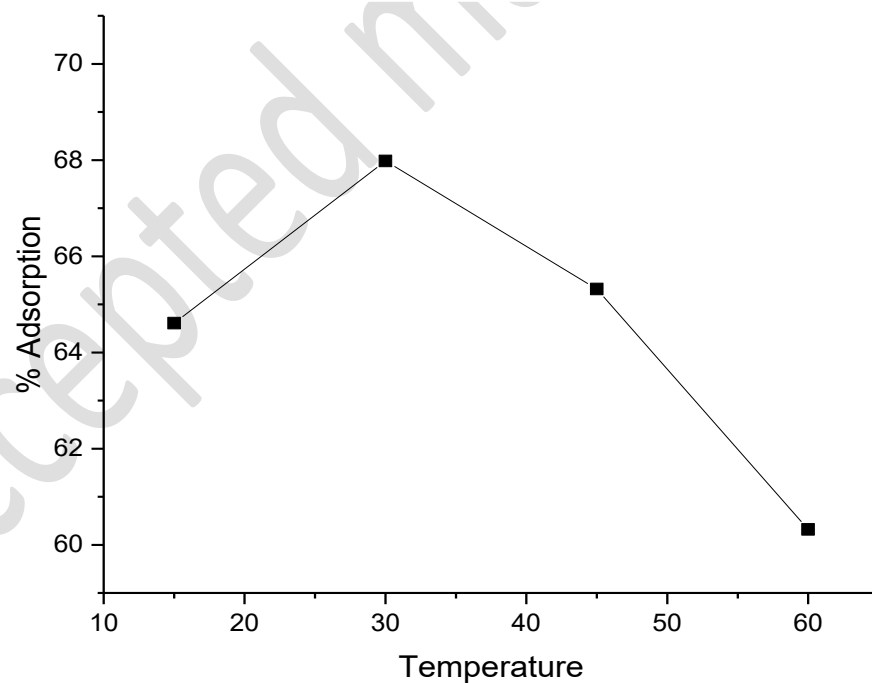


Figure 9 – Impact of chromium metal ion uptake by varying Temperature

Using the optimal pH of 2.0, an adsorbent dosage of 0.6 g/L, a starting ion concentration of 20 mg/L, and an 80-minute contact duration, the variations in metal ion uptake were investigated by

altering the temperature from 15 to 60°C. Figure 9 shows the variations in metal ion uptake by activated adsorbent material, and it was found to be rapid metal ion uptake when the solution temperature was very low. The solution's temperature was adjusted after the saturation point (30°C), and a sudden decrease in adsorption rate was noticed. The drop in chromium ion uptake after the saturation point indicates the rate of desorption that takes place (Priya et al, 2022).

3.10 Impact of chromium uptake by varying the particle size

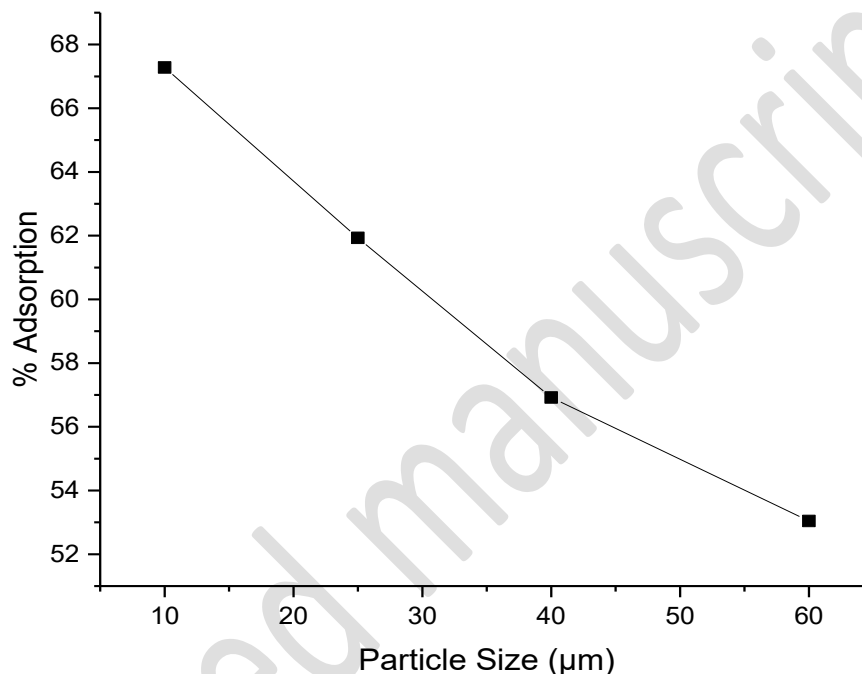


Figure 10 – Impact of chromium metal ion uptake by varying Particle Size

Adsorbent particle size variations are an important parameter in batch adsorption studies. The size of the adsorbent particle may affect the pollutant uptake from the aqueous solutions. In this study, the particle size of activated ZJ seeds adsorbent was adjusted to 10, 25, 40 & 65 μm, and the other parameters were taken from optimum conditions through batch studies. Figure 10 shows the variations in hexavalent chromium ion uptake by different activated ZJ adsorbent particle sizes. The maximum amount of chromium removal was achieved with the small particle size. i.e., 10 μm of adsorbent material received more hexavalent chromium ions because of its very high surface area and pore volume. The plot noticed a decrease in metal ion uptake when the particle size was increased. Metal ion uptake reduced as particle size increased due to limited active sites and surface area (Rico et al, 2018).

3.11 Isotherm studies

3.11.1 Langmuir isotherm study

The linear isotherm plot (C_e/q_e vs C_e) for the Langmuir study was shown in figure 11, and the constants of this isotherm model (k , q_{\max}) were obtained from slope and deflection values of linear plots and represented in table 3. The separation parameter obtained for chromium ions (0.0033) lies between 0 to 1, indicating a good adsorption process. Also, the calculated regression value (R^2) is more than 0.95 may confirm the applicability of this isotherm model, and the process of adsorption follows monolayer adsorption with heterogeneous nature (Biswas et al, 2015).

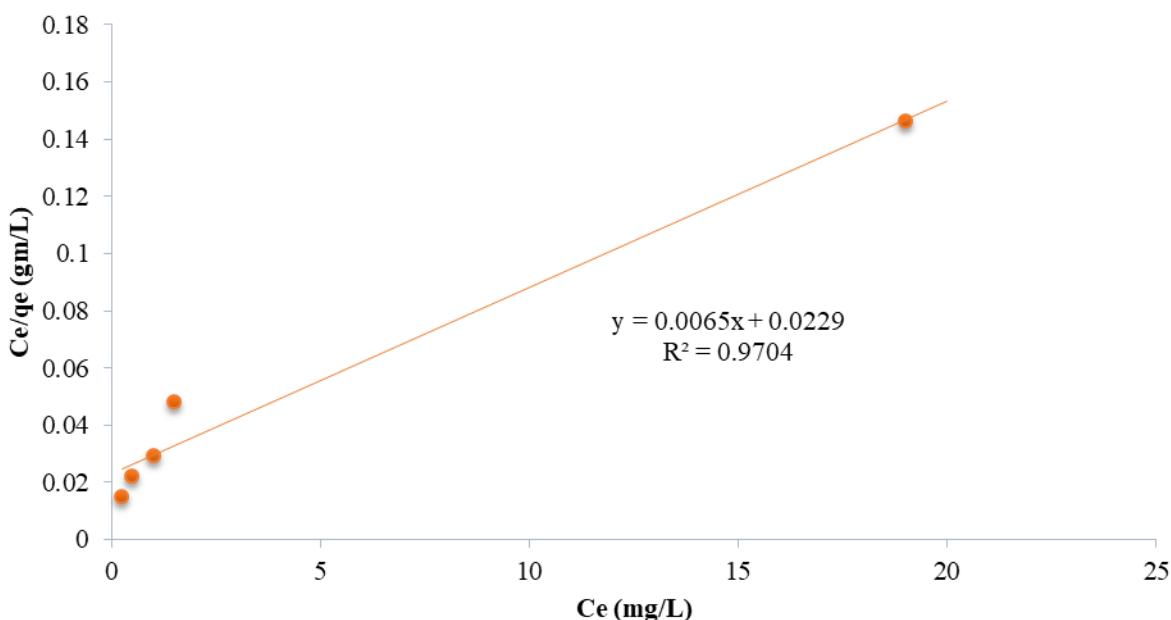


Figure 11 – Adsorption isotherm plots of Langmuir model for hexavalent chromium uptake using activated ZJ seeds powder

3.11.2 Freundlich isotherm study

The linear plot ($\ln q_e$ vs $\ln C_e$) of the Freundlich model was shown in figure 12, and the constants of this model (K_f & n) were obtained from the slope and deflection value of the plot, represented in table 3. The constant 'n' value obtained from the plot is 3.563, which lies between 1 to 10, which may confirm the physical adsorption process of chromium ions by the ZJ adsorbent. With the same set of experimental data, both Langmuir and Freundlich isotherm analysis was performed, and the regression values (R^2) were more than the expected level. Based on the

observations, it was confirmed the process of chromium uptake by the adsorbent follows the monolayer/multilayer adsorption process (Khan et al, 2022).

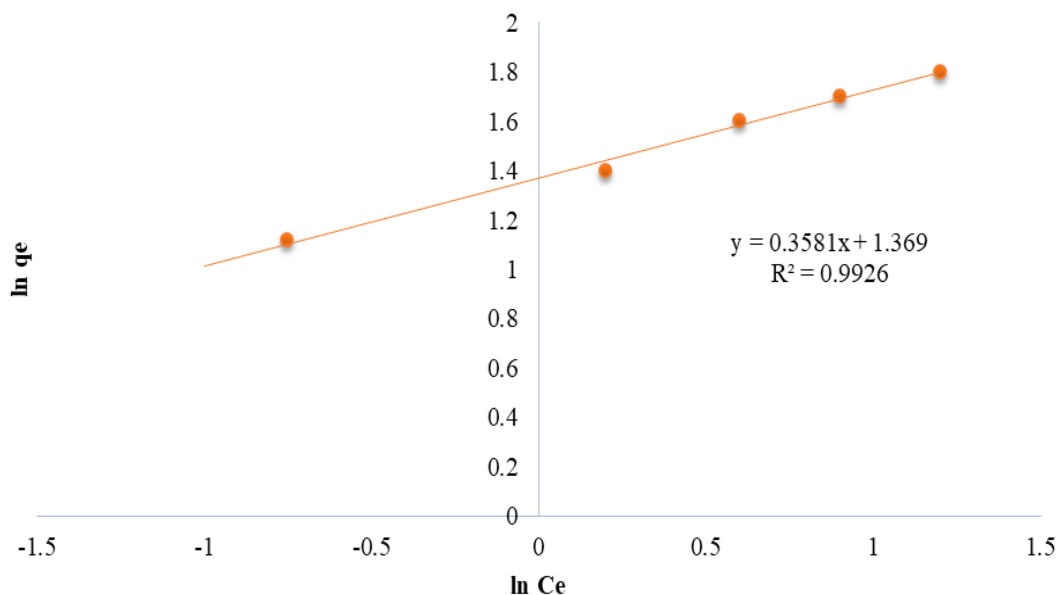


Figure 12 – Adsorption isotherm plots of Freundlich model for hexavalent chromium uptake using activated ZJ seeds powder

3.11.3 Sips isotherm study

Figure 13 shows the linear plot of the sips isotherm model, and the constants of this model (Q_{\max} & K_s) were obtained and represented in table 3. The heterogeneity factor (n) describes the fitting of Langmuir or Freundlich isotherm models, and the regression (R^2) value is more than 0.95, indicating the applicability of the sips isotherm study. If the n value reaches 1, this equation reduces to the Langmuir equation and infers the adsorption process in a homogeneous nature.

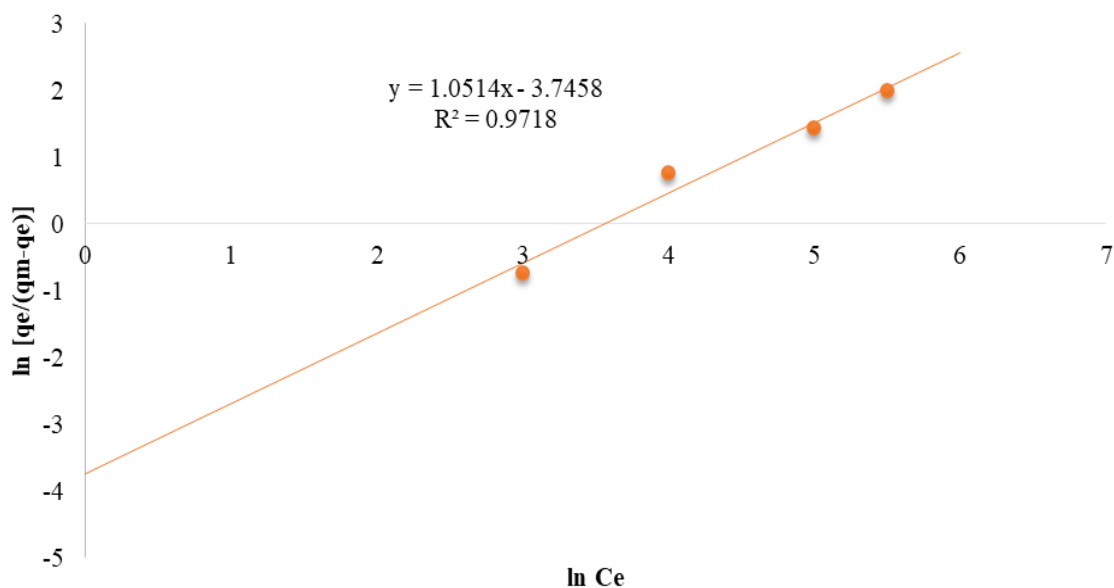


Figure 13 – Adsorption isotherm plots of Sips model for hexavalent chromium uptake using activated ZJ seeds powder

3.11.4 Toth isotherm study

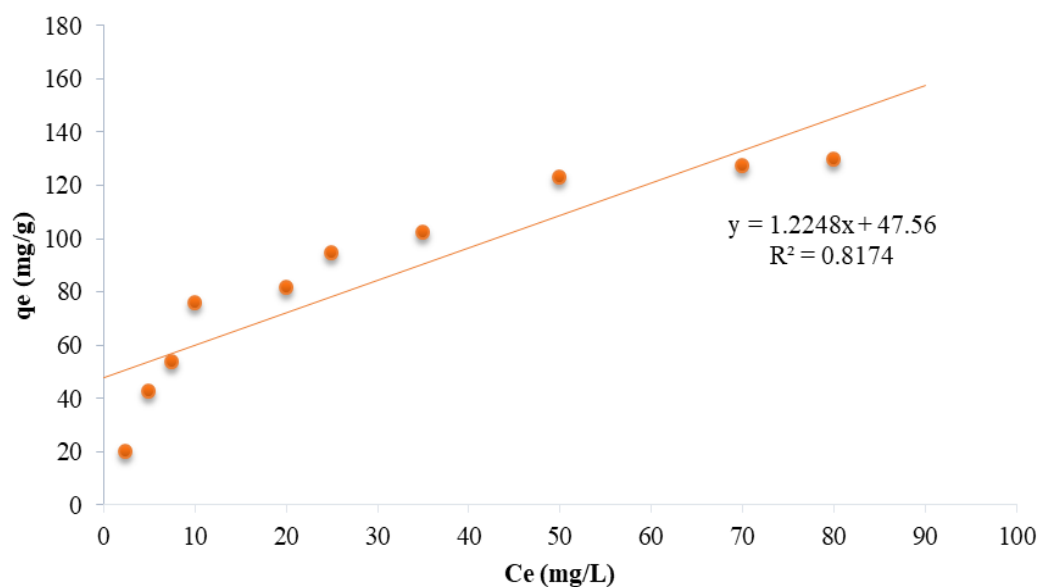


Figure 14 – Adsorption isotherm plots Toth model for hexavalent chromium uptake using activated ZJ seeds powder

Similar to previous studies, the linear plots were used to determine the constants of this kinetic model and are represented in table 3. Figure 14 shows the linear plot of the Toth isotherm model.

This model, also called a three-parameter model, provides more accuracy than other isotherm studies. To identify the heterogeneous solid surfaces, the Toth isotherm study was used (Edet et al, 2020). The regression value of this isotherm model was found to be very low ($R^2 < 1$), and this model was not suitable for the metal ion adsorption process. The Toth isotherm plots were used to connect the equilibrium data if the Langmuir isotherm was not fitted properly with the adsorption process.

3.11.5 R-P isotherm study

Figure 15 shows the linear plot of the R-P isotherm model, and the constants (K_R & a_R) were obtained from the linear plot and listed in table 3. The isotherm model has three unknown parameters, which provide high accuracy of results for the adsorption process. The regression value (R^2) is more than 0.95, confirming the fitting of this isotherm model, and the b_R values lie between 0 to 1, which represents the fitting of isotherm models. If the value of b_R is equal to 1, it becomes the Langmuir isotherm fit, and b_R equals 0, representing the Freundlich isotherm fitting method (Kromah et al, 2021).

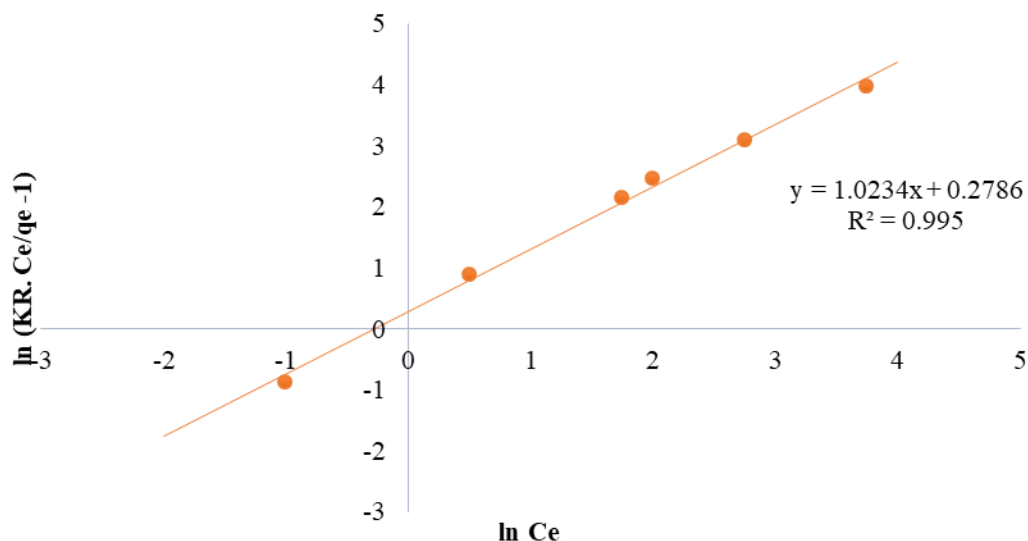


Figure 15 – Adsorption isotherm plots of R-P model for hexavalent chromium uptake using activated ZJ seeds powder

Table 3 – Adsorption isotherm constants for chromium adsorption using activated ZJ seeds powder

S. No.	Model	Parameters	Cr ⁶⁺ adsorption constants
1.	Langmuir	q_{\max}	9.402
		K_L	0.343
		R^2	0.9704
2.	Freundlich	K_f	2.541
		n	2.963
		R^2	0.9926
3.	Redlich-Peterson (R-P)	K_{RP}	11.325
		α_{RP}	0.3268
		β_{RP}	1.0521
		R^2	0.995
4.	Sips	K_S	12.868
		β_S	1.2534
		a_S	0.4734
		R^2	0.9718
5.	Toth	Q_{\max}	27.4598
		b_T	0.38393
		n_T	0.78414
		R^2	0.8714

3.12 Kinetic studies

3.12.1 Pseudo first order study

The first-order pseudoscience study described the chromium metal ion concentrations from 20 to 100 mg/L in the synthetic solutions and the kinetics of adsorption. The linear plots $((q_e - q) \& t)$ for the Lagergren study were shown in figure 16, and the kinetic & regression constants ($k \& R^2$) were obtained from the plots and listed in table 4. The regression values obtained from the plot are more than 0.95, indicating the Lagergren study's applicability for this adsorption process. Also, the process of adsorption reached the equilibrium level based on the regression indication (Venkatraman et al, 2022).

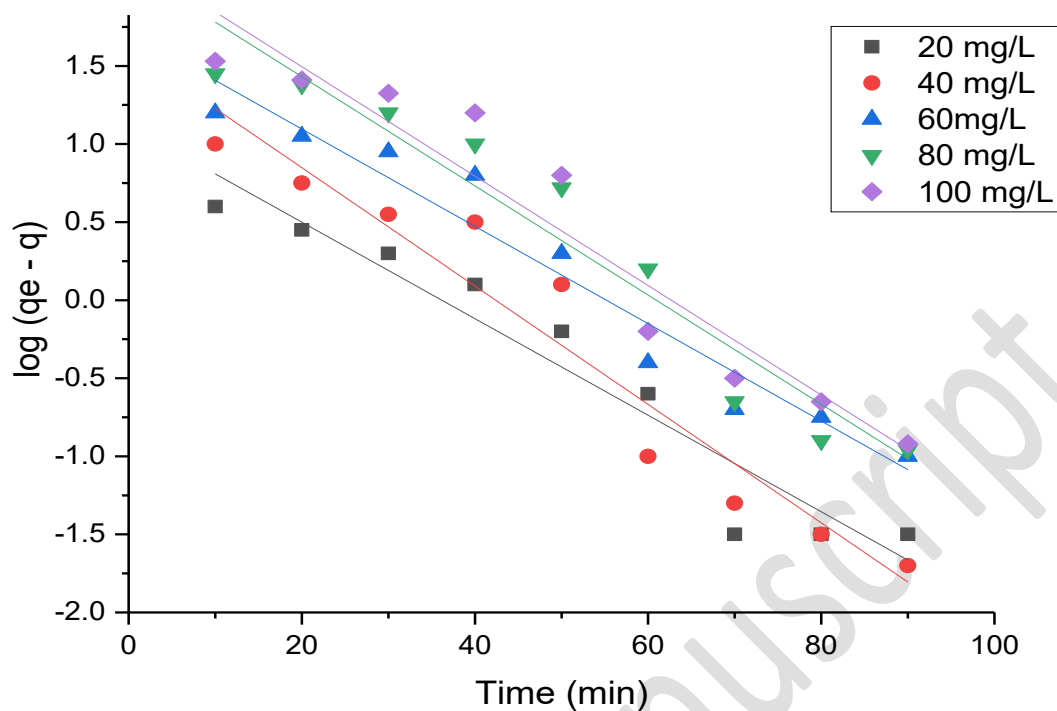


Figure 16 – Kinetic plots of Pseudo 1st order model for hexavalent chromium uptake using activated ZJ seeds powder

3.12.2 Pseudo second order study

The linear plot of this kinetic study (t/q vs t) was shown in figure 17, and the constants of this kinetic model were obtained from slope and deflection values in a linear plot. Like first-order studies, the concentration of chromium ion solution was adjusted, and the fitting of second-order studies was evaluated based on the regression values. The calculated q_e values are nearby the experimental q_e values and the regression values R^2 are more than 0.95, which indicates the applicability of this kinetic model and that the process of adsorption has reached the conditions of equilibrium (Zhang et al, 2019).

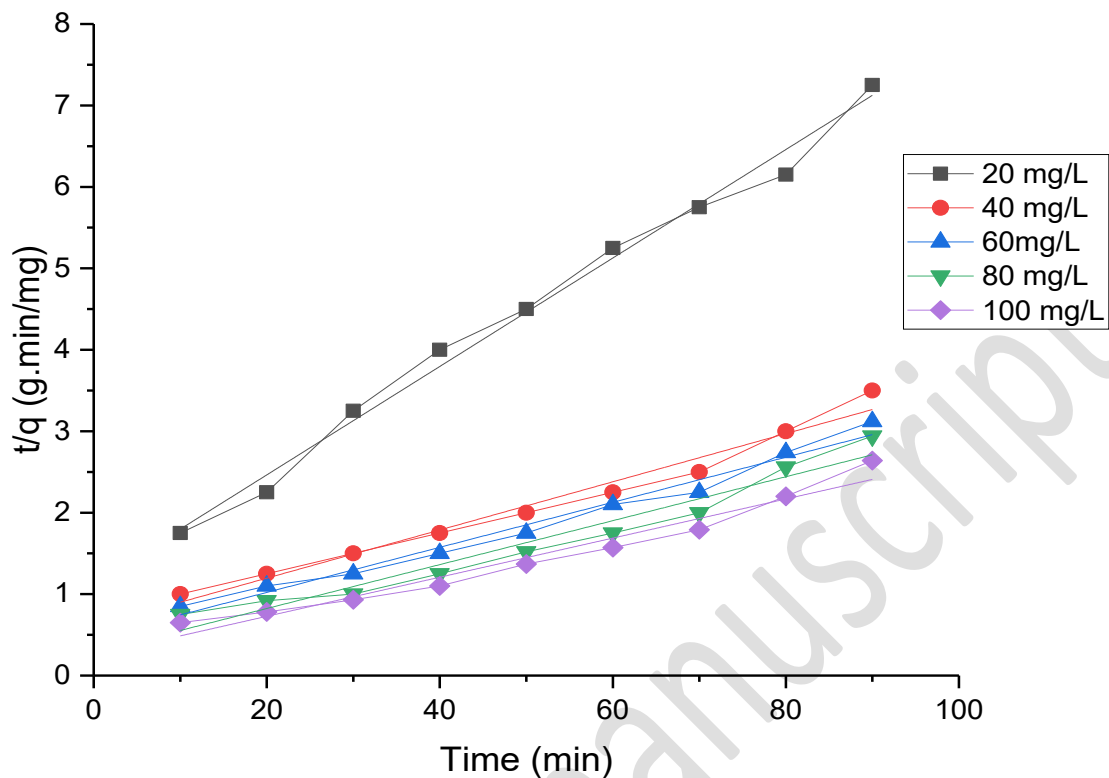


Figure 17 – Kinetic plots of Pseudo 2nd order model for hexavalent chromium uptake using activated ZJ seeds powder

3.12.3 Elovich kinetic study

The linear plots of the Elovich kinetic study (q_t vs $\ln(t)$) are shown in figure 18, and the constants (a and b) of this kinetic model are listed in table 4. Similar to the pseudo and second-order studies, the concentration of chromium ions was adjusted, and the performance of the Elovich model was evaluated. The R^2 value obtained from the linear plot was low, and the model was not fitted well with the adsorption process. This kinetic model does not predict any particular function, but it is used for clarifying the heterogeneous adsorbents in extreme conditions (Yogeshwaran et al, 2021). Because of the presence of heterogeneous active sites in activated ZJ seeds adsorbent, the Elovich kinetic model may also be used to determine the kinetics of metal ion adsorption during the entire adsorption period.

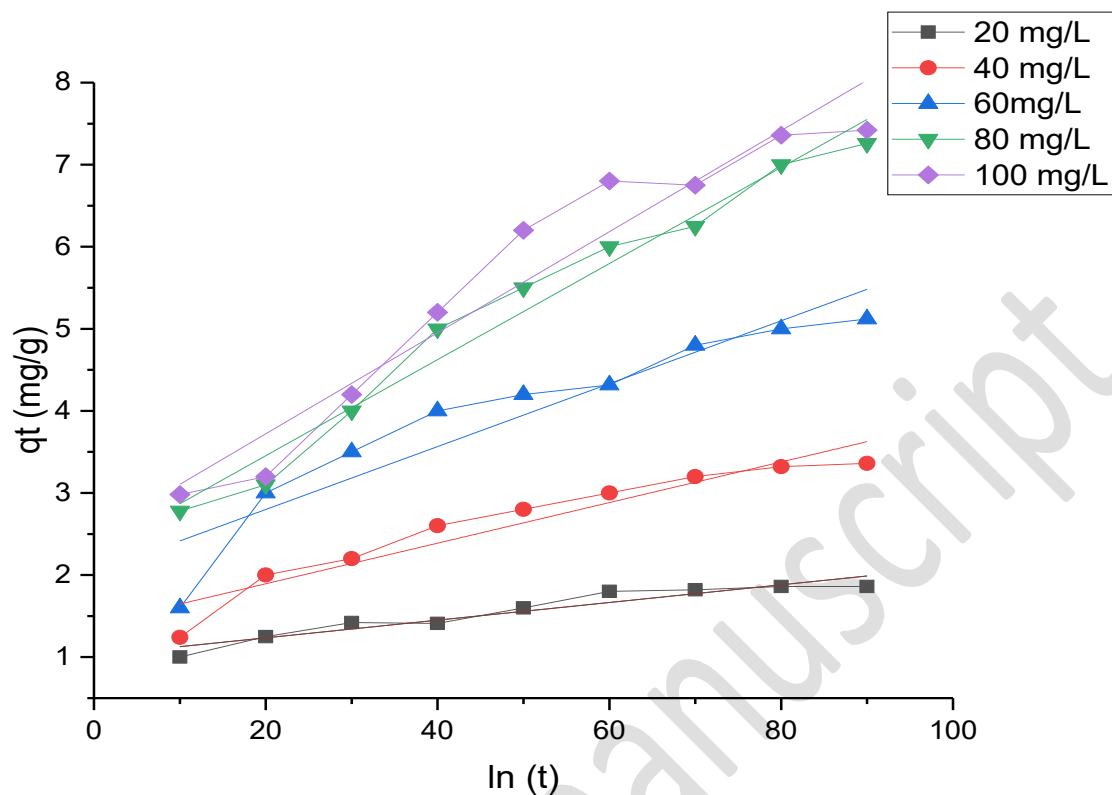


Figure 18 – Kinetic plots of Elovich model for hexavalent chromium uptake using activated ZJ seeds powder

Table 4 – Adsorption kinetic constants of Cr^{6+} uptake using activated ZJ seeds powder

S. No.	Conc. (mg/L)	Pseudo 1 st order			Pseudo 2 nd order				Elovich		
		K (min ⁻¹)	q _{e, cal} (mg/g)	R ²	K (g/mg. min) X 10 ⁻³	q _{e, cal} (mg/g)	h (mg/g. min)	R ²	a (mg/g. min)	b (g/mg)	R ²
1.	20	0.043	2.15	0.96	17.21	1.98	0.12	0.96	0.342	1.63	0.92
2.	40	0.056	6.95	0.97	13.59	4.89	0.16	0.98	0.783	0.92	0.94
3.	60	0.061	9.93	0.96	9.83	7.94	0.22	0.98	0.957	0.73	0.92
4.	80	0.049	12.68	0.96	4.36	9.87	0.25	0.98	0.931	0.48	0.94
5.	100	0.042	16.54	0.98	1.95	11.59	0.31	0.97	0.902	0.29	0.92

3.13 Thermodynamic studies

The chromium ion containing solution's concentration was adjusted from 20 to 100 mg/L, and the thermodynamic graphs for different metal ion concentrations are given in figure 19. The slope and intercept values (ΔH_o and ΔS_o) were calculated and represented in table 5. The values of ΔG_o (Gibbs Energy) found to be negative with positive ΔH_o (Enthalpy) values may confirm the reaction is endothermic because of the spontaneous nature of activated ZJ seeds powder (Malima et al, 2021). The uncertainty between solid and liquid phases was identified by referring to the positive ΔS_o (Entropy) values and their increases during the adsorption process in the aqueous medium (Kołodysńska et al, 2016)

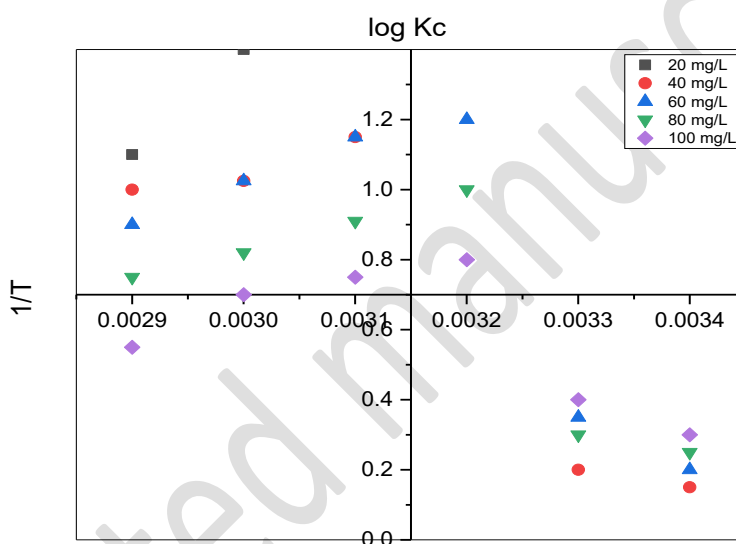


Figure 19 – Thermodynamic plot of Cr^{6+} adsorption using activated ZJ seeds powder

Table 5 – Thermodynamic constants of Cr^{6+} metal adsorption using activated ZJ seeds powder

Initial Cr^{6+} Concentration in Mg/L	Enthalpy (ΔH°) KJ/mol	Entropy (ΔS°) J/mol	Gibbs Energy (ΔG_o) kJ/mol			
			15°C	30°C	45°C	60°C
20	82.283	189.472	-14.192	-10.281	-8.922	-7.492
40	43.294	99.583	-10.348	-8.293	-6.239	-6.029
60	21.944	49.293	-8.593	-5.294	-5.029	-5.132
80	15.492	32.091	-5.291	-4.312	-3.924	-3.821
100	12.914	29.443	-3.982	-3.228	-3.012	-2.931

3.14 Desorption studies

Spent adsorbent disposal is one of the challenging problems in the adsorption process; also, it will create environmental pollution severely. Regeneration of spent adsorbent is the only way to make the adsorption process more economical (Fakhar et al, 2021). The hexavalent chromium metal ion recovery was made in desorption studies using concentrated hydrochloric acid with varying concentrations (0.1 to 0.4N). The number of chromium ions recovered from the spent adsorbent, and it was found the metal ion recovery was rapid during the initial time. The concentration of hydrochloric acid was increased by more than 0.3N, a sudden decrement in chromium recovery was observed, and it attained a constant rate. There was no increase in metal ion recovery with an increase in hydrochloric acid concentration, and the optimum value for chromium recovery was fixed by adding 0.3N of hydrochloric acid. The recovered metal ions were used in the different experimental processes. In this study, 0.3N of HCl acid took around 91.32% of chromium ions from the adsorbent surface.

4. CONCLUSION

The biosorption of hexavalent chromium ions was performed using activated ZJ seeds powder. At the ideal pH of 2.0, initial concentration of 20 mg/L, ZJ seeds dose of 0.6 g/L, and temperature of 30°C, the maximum adsorption efficiency of 63.23% was attained. FTIR, SEM, and EDX analysis confirmed the presence of targeted pollutants and the availability of functional groups in the activated ZJ seeds adsorbent. The adsorption process fit well with the Langmuir, Freundlich, R-P, and Sips isotherm models, and the adsorption approach follows Pseudo first and second order kinetic graphs. The thermodynamic studies confirm the exothermic nature of the adsorption process, and 0.3N of HCl desorbs 91.32% of spent chromium ions from the adsorbent. Based on the above studies, it was confirmed the ability of activated ZJ seed material to remove metal ion pollution from the aqueous solutions.

REFERENCES

1. Aderonke Ajibola Adeyemo, Idowu Olatunbosun Adeoye and Olugbenga Solomon Bello (2015). Adsorption of dyes using different types of clay: a review, Applied Water Science, 7, 543 – 568. <https://doi.org/10.1007/s13201-015-0322-y>
2. Alina Roxana Lucai, Dumitru Bulgariu, Maria-Christina Popescu and Laura Bulgariu (2020). Adsorption of Cu (II) ions on adsorbent materials obtained from marine red algae callithamnion corymbosum sp. Water, 12 (372). <http://dx.doi.org/10.3390/w12020372>

3. Amit Kumar Dey, Abhijit Dey and Rumi Goswami (2022). Adsorption characteristics of methyl red dye by Na₂CO₃-treated jute fibre using multi-criteria decision-making approach, *Applied Water Science*, 12, 179. <https://doi.org/10.1007/s13201-022-01700-9>
4. Batagarawa SM, Ajibola AK (2019). Comparative evaluation for the adsorption of toxic heavy metals on to millet, corn and rice husks as adsorbents. *Journal of Analytical and Pharmaceutical Research*, 3 , 119-125. Doi: [10.15406/japlr.2019.08.00325](https://doi.org/10.15406/japlr.2019.08.00325)
5. Bayuo J, Pelig-Ba K.B, Abukari M.A (2019) Adsorptive removal of chromium(VI) from aqueous solution unto groundnut shell. *Applied water science*, 9, 107. <https://doi.org/10.1007/s13201-019-0987-8>.
6. Biswajit sangha, Tarun kumar naiya, Ashim kumar bhattacharya, sudipkumar das (2011). Cr (VI) ions removal from aqueous solutions using natural adsorbents – FTIR studies. *Journal of environmental protection*, 2, 729 – 735. Doi: [10.4236/jep.2011.26084](https://doi.org/10.4236/jep.2011.26084)
7. Chawki Djelloul and Oualid Hamdaoui (2014). Dynamic adsorption of methylene blue by melon peel in fixed-bed columns, *Desalination and Water Treatment*, 56, 2966 – 2975. <https://doi.org/10.1080/19443994.2014.963158>
8. Dongxiao Ouyang, Yuting Zhuo, Liang Hu, Qiang Zeng, Yuehua Hu and Zhiguo He (2019). Research on the adsorption behaviour of heavy metal ions by porous material prepared with silicate tailings. *Minerals.*, 9, 291. Doi: [10.3390/min9050291](https://doi.org/10.3390/min9050291)
9. Edidiong D. Asuquo, Alastair D. Martin, Petrus Nzerem (2018). Evaluation of Cd (II) ion removal from aqueous solution by a low-cost adsorbent prepared from white yam (*Dioscorea rotundata*) waste using batch sorption. *Chemengineering*, 2 (35). Doi: [10.3390/chemengineering2030035](https://doi.org/10.3390/chemengineering2030035).
10. Francisco J. Alguacil and Felix A. Lopez (2020). Adsorption processing for the removal of toxic Hg (II) from liquid effluents: Advances in the 2019 year, *Metals*, 10 (3). <https://doi.org/10.3390/met10030412>
11. Hana Boubaker, Rim Ben Arfi, Karine Mougín, Cyril Vaultot, Samar Hajj, Philippe Kunneman, Gautier Schrodj and Achraf Ghorbal (2021). New optimization approach for successive cationic and anionic dyes uptake using reed-based beads, *Journal of Cleaner Production*, 307, 127218. <https://doi.org/10.1016/j.jclepro.2021.127218>
12. Jabbar H. Al – Baidhani, Simaa T. Al – Salihiy (2016). Removal of heavy metals from aqueous solution by using low cost rice husk in batch and continious fluidized experiments.

International Journal of Chemical Engineering and Applications, 7, 6 – 10.
<http://www.ijcea.org/vol7/532-P1003.pdf>

13. Jayachandran Sheeja, Krishnan Sampath and Ramasamy Kesavasamy (2021). Experimental Investigations on Adsorption of Reactive Toxic Dyes Using Hedyotis umbellate Activated Carbon, Adsorption Science and Technology, ID – 5035539.
<https://doi.org/10.1155/2021/5035539>
14. Jie Hong, Junyu Xie, Seyyedali Mirshahghassemi, Jamie Lead (2020). Metal (Cu, Cr, Ni, Pb) removal from environmentally relevant waters using polyvinylpyrrolidone – coated magnetic nanoparticles. RSC advances, 10, 3266 – 3276. Doi: <https://doi.org/10.1039/C9RA10104G>
15. K. Aswini, V. Jaishankar (2019). Adsorption treatment of heavy metal removal from simulated wastewater using rice husk activated carbon and its polyvinylpyrrolidone composite as an adsorbent. Journal of Water and Environmental Sciences, 3, 460 – 470.
<https://revues.imist.ma/index.php/jwes/article/view/12465/12658>
16. Luisa mayra vera, Daniel bermejo, Maria fernanda uguna, Marittza flores, Nancy garcia and Enrique Gonzalez (2018). Fixed bed column modelling of lead (II) and cadmium (II) ions biosorption on sugarcane bagasse. Environmental engineering research. Doi: <https://doi.org/10.4491/eer.2018.042>
17. Manjuladevi M, Anitha R, Manonmani S (2018). Kinetic study on adsorption of Cr (VI), Ni (II), Cd (II) and Pb (II) ions from aqueous solutions using activated carbon prepared from cucumis melo peel. Applied water science, 8, 36. Doi: <https://doi.org/10.1007/s13201-018-0674-1>.
18. Melánia Feszterová, Lýdia Porubcová and Anna Tirpáková (2021). The Monitoring of Selected Heavy Metals Content and Bioavailability in the Soil-Plant System and Its Impact on Sustainability in Agribusiness Food Chains, Sustainability, 13, 7021.
<https://doi.org/10.3390/su13137021>
19. Muhammad Mufazzal Saeed, Munir Ahmed (2020). Effect of temperature on kinetics and adsorption profile of endothermic chemisorption process: -tm (III) – PAN loaded PUF system. Separation science and technology, 41, 705 – 722. Doi: <https://doi.org/10.1080/01496390500527993>

20. Narges samadani langeroodi, Zhaleh farhadraresh, Aliakbar dehno khalaji (2018). Optimization of adsorption parameters for Fe (III) ions removal from aqueous solutions by transition metal oxide nanocomposite. Green chemistry letters and reviews, 11 (4), 404 – 413. Doi: <https://doi.org/10.1080/17518253.2018.1526329>
21. Priya A.K, Yogeshwaran V, Saravanan Rajendran, Tuan H.A. Hoang, Matias Soto – Moscoso, Ayman A. Ghfar and Chinna Bathula (2022). Investigation of mechanism of heavy metals (Cr^{6+} , Pb^{2+} & Zn^{2+}) adsorption from aqueous medium using rice husk ash: Kinetic and thermodynamic approach, Chemosphere, 286, 131796.
22. Rico I.L.R, Carrazana R.J.C, Karna N.K (2018). Modeling the mass transfer in biosorption of Cr (VI) y Ni (II) by natural sugarcane bagasse. Applied Water Science, 8, 55. <https://doi.org/10.1007/s13201-018-0692-z>
23. Swarup Biswas, Umesh Mishra (2015). Continious fixed bed column study and adsorption modeling: removal of lead ion from aqueous solution by charcoal originated from chemical carbonization of rubber wood sawdust. Journal of chemistry ID: 907379. Doi: <https://doi.org/10.1155/2015/907379>.
24. Tabrez Alam Khan, Md. Noumana, Divya Dua, Suhail Ayoub Khan, and Salman S. Alharthi (2022). Adsorptive scavenging of cationic dyes from aquatic phase by H_3PO_4 activated Indian jujube (*Ziziphus mauritiana*) seeds based activated carbon: Isotherm, kinetics, and thermodynamic study, Journal of Saudi Chemical Society, 26 (2), 101417. <https://doi.org/10.1016/j.jscs.2021.101417>
25. Uduakobong A. Edet, Augustine O (2020). Ifelebuegu, Kinetics, Isotherms, and Thermodynamic Modeling of the Adsorption of Phosphates from Model Wastewater Using Recycled Brick Waste. Processes, 8, 665.
26. Varney Kromah, Guanghui Zhang (2021). Aqueous Adsorption of Heavy Metals on Metal Sulfide Nanomaterials: Synthesis and Application. Water, 13, 1843.
27. Venkatraman Y and Priya A.K (2022). Removal of heavy metal ion concentrations from the wastewater using tobacco leaves coated with iron oxide nanoparticles. International Journal of Environmental Science and Technology, 19, 2721 – 2736.
28. Xiaoran Zhang, Shimin Guo, Jungfeg Liu, Ziyang Zhang, Kaihong Song, Chaohong Tan, Haiyan Li (2019). A study on the removal of copper (II) from aqueous solution using lime sand bricks. Applied Sciences, 9 (4), 670. Doi: <https://doi.org/10.3390/app9040670>

29. Yogeshwaran V and Priya A.K (2021). Experimental studies on the removal of heavy metal ion concentration using sugarcane bagasse in batch adsorption process. *Desalination and Water Treatment*, 224, 256 – 272. Doi: [10.5004/dwt.2021.27160](https://doi.org/10.5004/dwt.2021.27160)
30. Kumar Muthaiyan and R. Tamilarasan (2013). Kinetics, equilibrium data and modelling studies for the sorption of chromium by *Prosopis juliflora* bark carbon. *Arabian Journal of Chemistry*, 7 (S2). Doi: [10.1016/j.arabjc.2013.05.025](https://doi.org/10.1016/j.arabjc.2013.05.025)
31. Nyemaga Malima, Shesan John Owonubi, E. H. Lugwisha and A. S. Mwakaboko (2021). Thermodynamic, isothermal and kinetic studies of heavy metals adsorption by chemically modified Tanzanian Malangali kaolin clay. *International Journal of Environmental Science and Technology*, 18 (10), 1-16. <http://dx.doi.org/10.1007/s13762-020-03078-0>
32. Dorota Kołodyńska, Justyna Bąk and P. Thomas (2016). Comparison of Sorption and Desorption Studies of Heavy Metal Ions from Biochar and Commercial Active Carbon. *Chemical Engineering Journal*, 307. Doi: <http://dx.doi.org/10.1016/j.cej.2016.08.088>
33. Nida Fakhar, Suhail Ayoub Khan, Weqar Ahmad Siddiqi and Tabrez Alam Khan (2021). Ziziphus jujube waste-derived biomass as cost-effective adsorbent for the sequestration of Cd^{2+} from aqueous solution: Isotherm and kinetics studies. *Environmental Nanotechnology, Monitoring & Management*, 16, 100570. Doi: <https://doi.org/10.1016/j.enmm.2021.100570>
34. Radia Labied, Oumessaad Benturki, Adh' Ya Eddine Hamitouche and Andre' Donnot (2018). Adsorption of hexavalent chromium by activated carbon obtained from a waste lignocellulosic material (*Ziziphus jujuba* cores): Kinetic, equilibrium, and thermodynamic study. *Adsorption Science and Technology*, 36 (3-4), 1066-1099. Doi: [10.1177/0263617417750739](https://doi.org/10.1177/0263617417750739)
35. Nadir Khan, Fazal Wahid, Qamar Sultana, Najm Us Saqib and Muhammad Rahim (2020). Surface oxidized and un-oxidized activated carbon derived from *Ziziphus jujube* Stem, and its application in removal of Cd (II) and Pb (II) from aqueous media. *SN Applied Sciences*, 2, 753. Doi: <https://doi.org/10.1007/s42452-020-2578-6>
36. P. Ziarati, B. Farasati Far, E. Mashayekhi and B. Sawicka (2019). Removing arsenic by food processing waste (*Ziziphus Jujuba* seeds) and study on its adsorption properties. *Scientific and technical journal «Technogenic and Ecological Safety»*, 5, 62-70. <http://repositsc.nuczu.edu.ua/bitstream/123456789/8742/1/62-70-Parisa%20Ziarati.pdf>

37. Hadj Daoud Bouras, Oumessaâd Benturki, Noureddine Bouras, Mouloud Attou, André Donnot, André Merlin, Fatima Addoun and Michael D. Holtz (2015). The use of an agricultural waste material from *Ziziphus jujuba* as a novel adsorbent for humic acid removal from aqueous solutions. *Journal of Molecular Liquids*, 211, 1039 – 1046. Doi: <https://doi.org/10.1016/j.molliq.2015.08.028>
38. Abdelmajid Regti1, My Rachid Laamari, Salah-Eddine Stiriba and Mohammadine El Haddad (2017). The potential use of activated carbon prepared from *Ziziphus* species for removing dyes from waste waters. *Applied Water Science*, 7, 4099 – 4108. Doi: <https://doi.org/10.1007/s13201-017-0567-8>